



Surface-hydrophobized TEMPO-nanocellulose/rubber composite films prepared in heterogeneous and homogeneous systems

Shunsuke Fukui · Takuro Ito · Tsuguyuki Saito  · Toru Noguchi · Akira Isogai 

Received: 21 August 2018 / Accepted: 2 November 2018 / Published online: 11 November 2018
© Springer Nature B.V. 2018

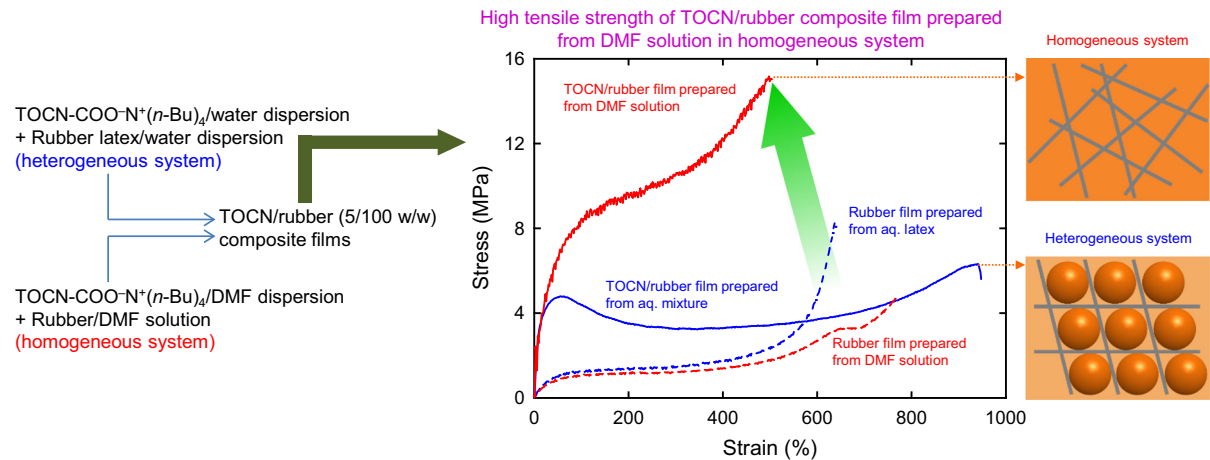
Abstract A surface-carboxylated nanocellulose was prepared from wood cellulose by catalytic oxidation with 2,2,6,6-tetramethylpiperidine-1-oxyl radical (TEMPO). The fibrous TEMPO-oxidized cellulose with sodium carboxylate groups (TOC-Na) was surface-hydrophobized by counterion exchange with tetra-*n*-butylammonium [TOC-N(*n*-Bu)₄]. This fibrous TOC-N(*n*-Bu)₄ was mechanically disintegrated in water and *N,N*-dimethylformamide (DMF) to prepare dispersions of TEMPO-oxidized cellulose nanofibrils (TOCNs) with tetra-*n*-butylammonium counterions, i.e., TOCN-N(*n*-Bu)₄/water and TOCN-N(*n*-Bu)₄/DMF. TOCN-N(*n*-Bu)₄/rubber composite films were prepared by mixing TOCN-N(*n*-Bu)₄ and hydrogenated acrylonitrile–butadiene rubber (H-NBR), used as a polymer matrix, in heterogeneous and homogeneous systems with water and DMF, respectively, followed by casting and drying. The TOCN-N(*n*-Bu)₄/H-NBR composite films prepared in

the heterogeneous and homogeneous systems both had a high Young's modulus of ~ 45 MPa and low coefficients of thermal expansion of ~ 20 ppm/K at a TOCN/H-NBR ratio of 5/100 (w/w). In contrast, the tensile strengths and strain-to-failure values of the composite films prepared using the two systems clearly differed. These different properties are probably caused by differences between the TOCN distributions in the H-NBR matrix and between the H-NBR matrix structures in the two systems. The composite films prepared in the homogeneous system with DMF as the medium are likely to have a more homogeneous distribution of TOCN elements in a homogeneous H-NBR polymer matrix, resulting in a higher tensile strength and work-of-fracture at TOCN/H-NBR = 5/100 (w/w) compared with those of the films prepared in the heterogeneous system with water.

S. Fukui · T. Ito · T. Saito · A. Isogai (✉)
Department of Biomaterial Sciences, The University of
Tokyo, Bunkyo-ku, Tokyo 113-8657, Japan
e-mail: aisogai@mail.ecc.u-tokyo.ac.jp

T. Noguchi
Institute of Carbon Science and Technology, Shinshu
University, Nagano 380-8553, Japan

Graphical abstract



Keywords TEMPO-nanocellulose · Hydrogenated acrylonitrile rubber · Composite film · Homogeneous system · Necking

Introduction

Nanocelluloses are promising bio-based nanomaterials. They can be used as both nanofillers to reinforce polymer matrices and versatile bulk materials such as transparent films, hydrogels, and aerogels (Habibi et al. 2010; Klemm et al. 2011; Moon et al. 2011; Isogai et al. 2011; Isogai 2013). Natural and synthetic rubbers have unique properties and are used as components of a wide range of products, including tires, belts, hose pipes, packings, sealants, O-rings, rollers, and cushions. The mechanical properties of rubbers are improved by vulcanization and addition of fillers such as carbon black and silica (Karasek and Sumita 1996; Hshim et al. 1998; Wang 1998). The reinforcement of rubbers with various nanofillers such as nanoclays (Varghese and Karger-Kocsis 2003; Gatos et al. 2005; Kader et al. 2006) and carbon nanotubes (Endo et al. 2008; Deng et al. 2011) has been investigated in recent years. Nanocelluloses have also been used as fillers for rubber matrix reinforcement (Bendahou et al. 2010; Bras et al. 2010; Abraham et al. 2013; Annamalai et al. 2014; Parambath Kanoth et al. 2015), and nanocellulose/rubber composite materials with good mechanical and thermal properties have been reported.

When plant cellulose/water suspensions at pH 10 are subjected to catalytic oxidation using 2,2,6,6-tetramethylpiperidine-1-oxyl (TEMPO) and NaBr with NaClO as the primary oxidant, significant amounts of sodium carboxylate groups are formed densely, regularly, and position-selectively on the crystalline cellulose microfibrils in the plant cellulose fibers. The mechanical disintegration of fibrous TEMPO-oxidized plant celluloses with carboxylate contents > 1 mmol/g in water under moderate conditions gives highly viscous and transparent gels. The gels consist of completely individualized TEMPO-oxidized cellulose nanofibrils (TOCNs) with homogeneous widths of ~ 3 nm and high aspect ratios, i.e., > 150, the morphologies of which are different from those of other nanocelluloses (Saito et al. 2006; 2007; Isogai et al. 2011; Shinoda et al. 2012). Moreover, because there are significant amounts of sodium carboxylate groups on the surfaces of the crystalline TOCN elements, other metal ions and hydrophobic alkylammonium ions can be introduced onto the TOCN surfaces by simple ion exchange in water (Fujisawa et al. 2012a, b, 2014; Shimizu et al. 2014a, b, 2016).

TOCN films prepared from TOCNs with sodium carboxylate groups (TOCN-Na) by casting and drying have high Young's moduli of 6–7 GPa, high tensile strengths of 200–300 MPa, low coefficients of thermal expansion (CTEs) of ~ 3 ppm/K, and low oxygen transmission rates of ~ 0.001 mL μm/(m² day kPa) under dry conditions (Fukuzumi et al. 2009; Isogai et al. 2011). The thermal and mechanical properties of

TOCN-reinforced rubber composite films are therefore expected to be better than those of neat rubber films or other nanocellulose-reinforced composite rubber films because TOCNs have higher aspect ratios and more homogeneous and smaller widths than other nanocelluloses. When counterion-exchanged TOCNs (TOCN-X) and surface-hydrophobized TOCNs were used as fillers to reinforce polystyrene, poly(lactic acid), and cellulose triacetate matrices, the mechanical and thermal properties of the TOCN/polymer composite films were significantly better than those of the neat polymer films (Fujisawa et al. 2012a, b, 2014; Soeta et al. 2015).

In a previous study, TOCN-X was mixed with hydrogenated acrylonitrile–butadiene rubber (H-NBR) latex under aqueous conditions, followed by casting and drying to prepare TOCN-X/H-NBR (TOCN/H-NBR = 0–5/100, w/w) composite films. H-NBR is a high-performance polymer, with better oil resistance, thermal resistance, and weather resistance than other natural and synthetic rubbers (Aimura 1997). The TOCN-X/H-NBR (TOCN/H-NBR = 5/100, w/w) composite films had high Young's moduli, high storage elastic moduli at temperatures above the glass-transition point, and low CTEs under dry nitrogen conditions. However, microscopy images show that the hydrophilic TOCN elements form heterogeneous grid-like networks around hydrophobic H-NBR latex particles in the composite films. If TOCN/H-NBR composite films are prepared using surface-hydrophobized TOCNs in a homogeneous system using an H-NBR/organic solvent solution (rather than the aqueous H-NBR latex described above), TOCN/H-NBR composite films with different mechanical or thermal properties should be obtained.

In this study, surface-hydrophobized TOCN/H-NBR composite films were prepared in heterogeneous system with water and a homogeneous system with *N,N*-dimethylformamide (DMF). The mechanical and thermal properties of TOCN/rubber composite films prepared using the two systems were compared to clarify the effects of different preparation systems on the TOCN/H-NBR composite film properties.

Experimental

Materials

TEMPO-oxidized cellulose with a sodium carboxylate content of 1.1 mmol/g (TOC-Na) was prepared from wood cellulose according to a previously reported procedure (Fukui et al. 2018). A commercial H-NBR latex (solid content 40%, w/v, Zetpol 2230LX, Nippon Zeon Co., Ltd., Tokyo, Japan) was kindly provided by Nippon Zeon. The chemical structure of H-NBR is shown in Fig. 1. The aqueous H-NBR latex (2 mL) was freeze-dried, and the freeze-dried H-NBR was stirred in DMF (20 mL) to prepare a 4% (w/v) H-NBR/DMF solution. Aqueous $N(n\text{-Bu})_4\text{OH}$ solution was purchased from Sigma-Aldrich (USA). Other chemicals and solvents (laboratory grade, Wako Pure Chemical Ind. Ltd., Osaka, Japan) were used as received.

Preparation of TEMPO-oxidized cellulose nanofibrils

TOCNs with tetra-*n*-butylammonium counterions [TOCN- $N(n\text{-Bu})_4$] were prepared from fibrous TOC-Na. The TOC-Na was counterion-exchanged to TOC-H with 1 M HCl, and the TOC-H was counterion-exchanged to TOC- $N(n\text{-Bu})_4$ by neutralization with $N(n\text{-Bu})_4\text{OH}$ (Shimizu et al. 2014a; Fukui et al. 2018). The TOC- $N(n\text{-Bu})_4$ was mechanically disintegrated in water using double-cylinder-type and ultrasonic homogenizers under the conditions reported in a previous paper (Fukui et al. 2018). The fibrous TOC- $N(n\text{-Bu})_4$ /water suspension was solvent exchanged to give a TOC- $N(n\text{-Bu})_4$ /DMF suspension by centrifugation several times with fresh DMF. The TOC- $N(n\text{-Bu})_4$ /DMF suspension was mechanically disintegrated to give a TOCN- $N(n\text{-Bu})_4$ /DMF dispersion. The TOCN- $N(n\text{-Bu})_4$ /water and TOCN- $N(n\text{-Bu})_4$ /DMF dispersions were both centrifuged at $12,000\times g$ for 10 min to remove the small amounts of unfibrillated fractions. The supernatants were used as $\sim 0.1\%$ (w/v) TOCN- $N(n\text{-Bu})_4$ /water and TOCN- $N(n\text{-Bu})_4$ /DMF dispersions.

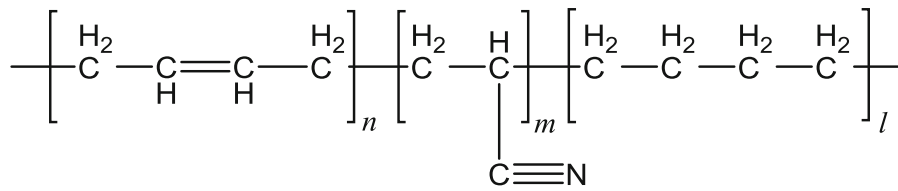


Fig. 1 Chemical structure of hydrogenated acrylonitrile–butadiene rubber (H-NBR)

Preparation of TOCN-N(*n*-Bu)₄/H-NBR composite films

Certain amounts of TOCN-N(*n*-Bu)₄/water dispersion were added to aqueous H-NBR latex (2 mL). The mixtures were stirred for 30 min, cast in glass Petri dishes, and dried at 40 °C for 3 days to prepare TOCN-N(*n*-Bu)₄/H-NBR composite films with TOCN/H-NBR weight ratios of 0–5/100 (without including the weights of the TOCN counterions) in the heterogeneous TOCN/H-NBR latex/water system (Fig. 2a). Certain amounts of TOCN-N(*n*-Bu)₄/DMF dispersion were added to the H-NBR/DMF solution, and the mixtures were stirred for 30 min. The mixtures were then cast in glass Petri dishes, and dried in vacuo at 60 °C for 3 days to prepare TOCN-N(*n*-Bu)₄/H-NBR (TOCN/H-NBR = 0–5/100, w/w) composite films using a homogeneous TOCN/H-NBR/DMF system (Fig. 2b). The neat and composite film thicknesses and densities after conditioning at 23 °C and 50% relative humidity were ~ 200 μm and 0.8–0.9 g/cm³, respectively.

Analyses

Light-transmittance spectra of the composite films were recorded from 400 to 800 nm using a spectrophotometer (V-670, JASCO Corp., Tokyo, Japan) (Fukui et al. 2018). Tensile tests and thermomechanical analysis of the composite films were performed according to previously reported methods (Fukui et al. 2018).

Results and discussion

Preparation of TOCN-N(*n*-Bu)₄/H-NBR composite films

All the TOCN-N(*n*-Bu)₄/H-NBR composite films prepared in the heterogeneous system with water had high light transparencies, i.e., ~ 80% at 600 nm wavelength, similar to those reported for TOCN-Na/H-NBR composite films prepared in the same heterogeneous system with water (Fukui et al. 2018). In contrast, the composite films prepared in the homogeneous system with DMF had low transparencies (Fig. 3). This may have been the result of light scattering from the relatively rough surfaces of the films prepared using the homogeneous system; composite films prepared in the heterogeneous system had smooth surfaces (see photographs in Fig. 2). Another possibility is that the small amount of surfactant present in the original H-NBR latex to improve the stability of the latex particles in water, which is present in the freeze-dried H-NBR, is insoluble in DMF or immiscible with the TOCN-N(*n*-Bu)₄ and H-NBR components of the films.

Mechanical properties of TOCN-N(*n*-Bu)₄/H-NBR composite films

Typical stress–strain curves for the composite films prepared in the heterogeneous and homogeneous systems are shown in Fig. 4. The relationships between the TOCN content and the Young’s modulus, tensile strength, strain-to-failure, and work-of-fracture were calculated from the stress–strain curves in Fig. 4 and plotted in Fig. 5. The TOCN-N(*n*-Bu)₄/H-NBR (TOCN/H-NBR = 5/100, w/w) composite film showed a clear yield phenomenon in the stress–strain curve.

As shown in Fig. 5, the Young’s moduli of the composite films prepared in the two systems increased

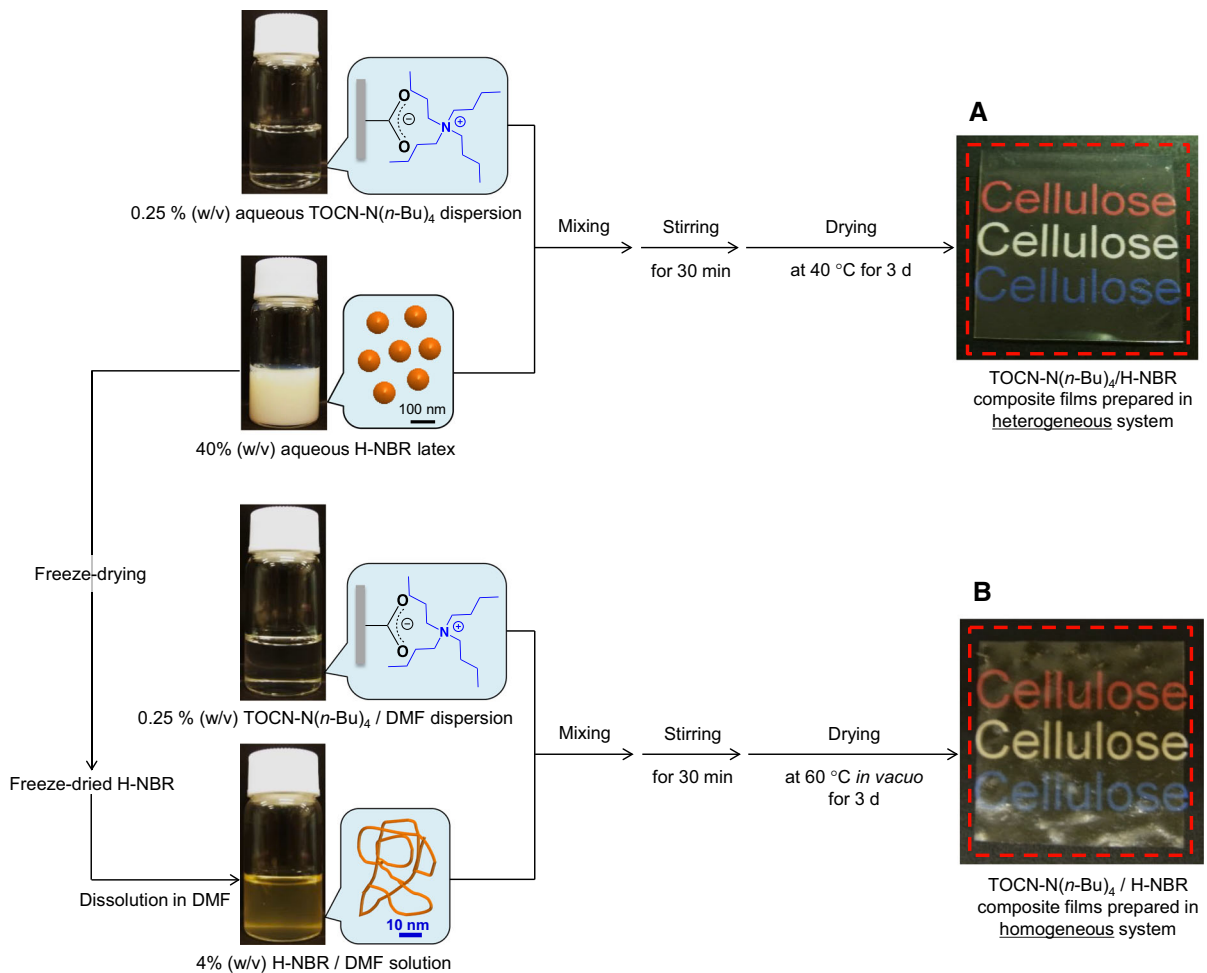


Fig. 2 Schematic diagrams of preparation of TOCN-N(*n*-Bu)₄/H-NBR composite films in heterogeneous system with water (a) (Fukui et al. 2018) and homogeneous system with DMF (b)

similarly with increasing TOCN content. There was almost no difference between the Young's moduli of the composite films prepared using the two systems at the same TOCN content. The tensile strengths of the composite films prepared in the heterogeneous system gradually decreased with increasing TOCN content, whereas those of the composite films prepared in the homogeneous system increased. Conversely, the strain-to-failure values of the composite films prepared in the heterogeneous system increased with increasing TOCN content, whereas those of the composite films prepared in the homogeneous system decreased. The work-of-fracture values increased with increasing TOCN content for the composite films prepared in the two systems, although the values were different for films prepared in the two systems at the

same TOCN content. The trends in the tensile strengths and strain-to-failure values of the composite films prepared in the two systems therefore clearly differed.

Thermal properties of TOCN-N(*n*-Bu)₄/H-NBR composite films

The CTE values in temperature regions A and B in Fig. 6 were calculated by plotting the expansion ratios of the composite films against temperature under dry nitrogen conditions. The CTEs of the composite films prepared in the two systems decreased significantly with increasing TOCN content in the temperature regions A and B in Fig. 6. No significant differences were observed between the CTE values for the

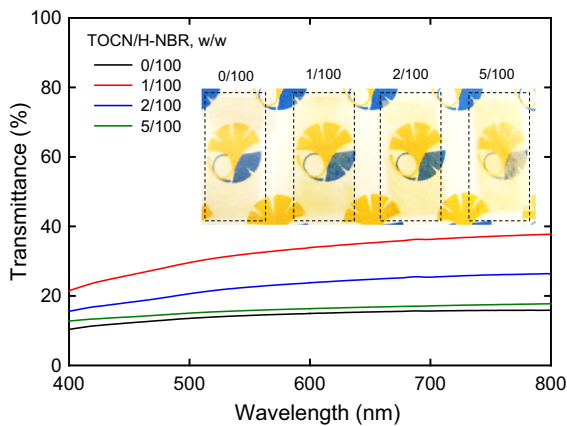


Fig. 3 Light-transmittance spectra of TOCN-N(*n*-Bu)₄/H-NBR (TOCN/H-NBR = 0–5/100, w/w) composite films prepared in homogeneous system with DMF (Fig. 2b). Inset shows photographs of corresponding composite films

composite films prepared in the two systems in the lower temperature range A.

Difference between structures of composite films prepared in heterogeneous and homogeneous systems

As described in the previous section, there were clear differences between the tensile strengths and strain-to-failure values of the TOCN-N(*n*-Bu)₄/H-NBR (TOCN/H-NBR = 5/100, w/w) composite films prepared in the heterogeneous and homogeneous systems. The Young's moduli and CTE values of the composite films were almost the same at the same TOCN content.

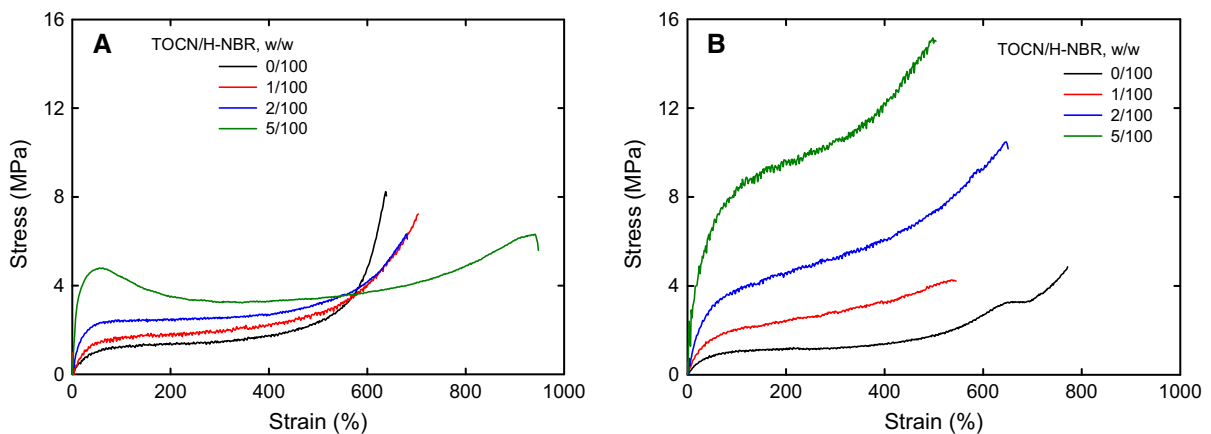


Fig. 4 Stress–strain curves for TOCN-N(*n*-Bu)₄/H-NBR composite films (with TOCN/H-NBR = 0–5/100, w/w) prepared in heterogeneous system with water (a) and homogeneous system with DMF (b)

Figures 7 and 8 show typical stress–strain curves for the TOCN-N(*n*-Bu)₄/H-NBR (TOCN/H-NBR = 5/100, w/w) composite films prepared in the heterogeneous system with water and homogeneous system with DMF, respectively, and the corresponding photographs of the films during tensile tests. The composite film prepared in the heterogeneous system showed a typical yield phenomenon and necking behavior. In contrast, the composite film prepared in the homogeneous system showed neither necking behavior nor yield during tensile tests. These results show that the primary differences between the two systems did not appear in the elastic region, unlike the Young's modulus or CTE, but appeared in the plastic region after the elastic region during tensile tests.

Necking behavior of polymer and polymer composite films in the plastic region during tensile tests has been studied experimentally and theoretically for a long time (Bucknall and Smith 1965; Wu and van der Giessen 1995; Brüning 1998; Tervoort and Govaert 2000). Polymer/clay composite films, which consist of spherical polymer particles surrounded with clay nanoparticles, show characteristic necking behavior during tensile tests (Haraguchi et al. 2006). A transmission electron microscopy image of the TOCN-N(*n*-Bu)₄/H-NBR (TOCN/H-NBR = 5/100, w/w) composite film showed that similar heterogeneous and two-phase structures may have been partly retained in the film (Fukui et al. 2018). When cellulose nanocrystals are homogeneously distributed in a rubber matrix, no necking behavior is observed during tensile tests (Nair and Dufresne 2003; De and White 1996). The results

Fig. 5 Relationships between TOCN content and Young's modulus, tensile strength, strain-to-failure, and work-of-fracture of composite films prepared in heterogeneous system with water and homogeneous system with DMF

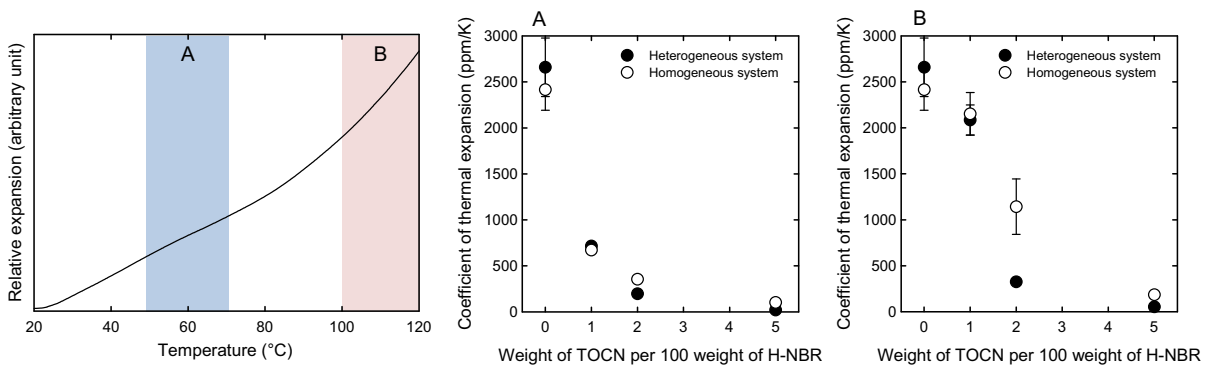
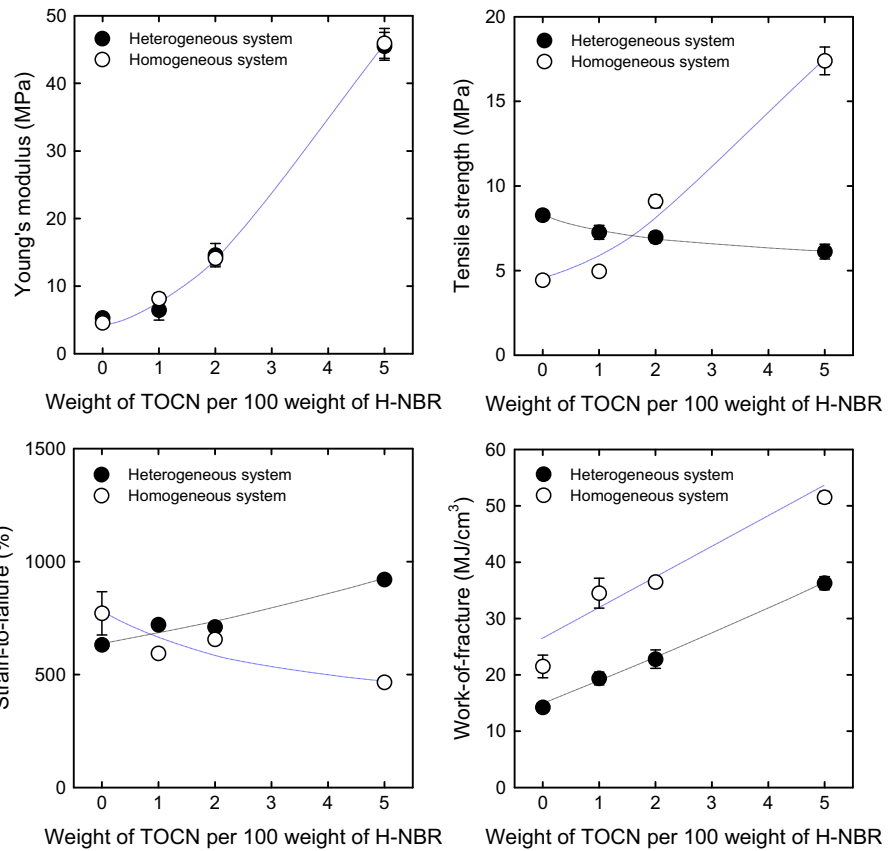


Fig. 6 Typical thermal expansion curve for composite film (left), and relationships between TOCN contents and coefficient of thermal expansion of TOCN-N(*n*-Bu)₄/H-NBR composite film in temperature regions A and B

shown in Figs. 7 and 8 therefore suggest that TOCN-N(*n*-Bu)₄ elements are homogeneously distributed in a homogeneous H-NBR polymer matrix in the composite film prepared in the homogeneous system with DMF.

Figure 9 shows typical stress–strain curves in first and second tensile tests; the second tensile test was

performed before the point at which fracture occurred in the first test for the same sample specimen. Neither a yield phenomenon nor necking behavior was observed in the second tensile test for the composite film prepared in the heterogeneous system. The originally heterogeneous and two-phase structures of the TOCN-N(*n*-Bu)₄/H-NBR composite film prepared in the

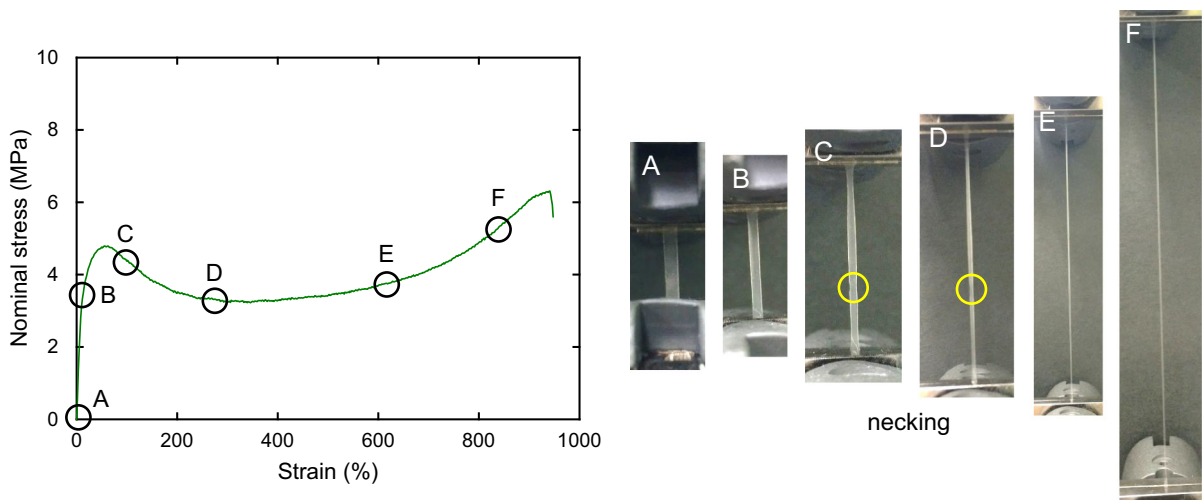


Fig. 7 Typical stress–strain curve for TOCN- $N(n\text{-Bu})_4$ /H-NBR (TOCN/H-NBR = 5/100, w/w) composite film prepared in heterogeneous system with water, and photographs of film during tensile test, showing necking behavior at C and D

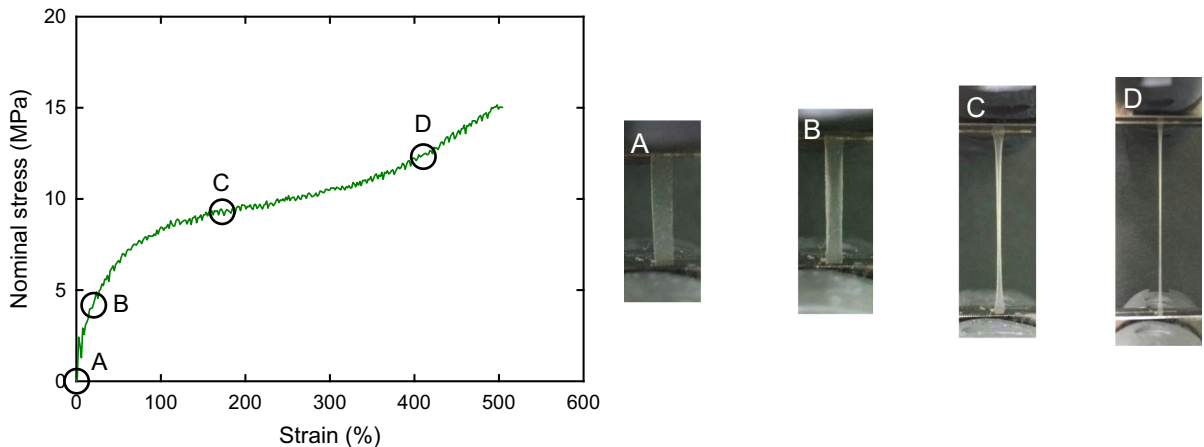


Fig. 8 Typical stress–strains curve for TOCN- $N(n\text{-Bu})_4$ /H-NBR (TOCN/H-NBR = 5/100, w/w) composite film prepared in homogeneous system with DMF, and photographs of film during tensile test, showing no necking behavior

heterogeneous system therefore became more homogeneous, similar to those of the composite film prepared in the homogeneous system. However, the tensile strength and strain-to-failure value of the composite film prepared in the homogeneous system, determined in the second tensile test (Fig. 9b), were still much higher and lower, respectively, than those for the composite film shown in Fig. 9a.

Schematic structural models of the TOCN- $N(n\text{-Bu})_4$ /H-NBR composite films prepared in the two systems are shown in Fig. 10. The procedure for preparation of the composite films in the heterogeneous system with water, without any organic solvent,

is much simpler and preferable to that for preparation in the homogeneous system with DMF, both environmentally and industrially. However, the homogeneous system is better for the preparation of TOCN/H-NBR composite films with high tensile strengths and more homogeneous structures. Thermal molding or kneading of aqueous dispersions of TOCNs and aqueous H-NBR latex is a simpler and more practical method for removing water from mixtures and preparing dry TOCN/H-NBR composite materials. However, in this case, hydrophilic TOCN elements aggregate preferentially in the hydrophobic H-NBR matrix during water removal, and the TOCNs have almost no

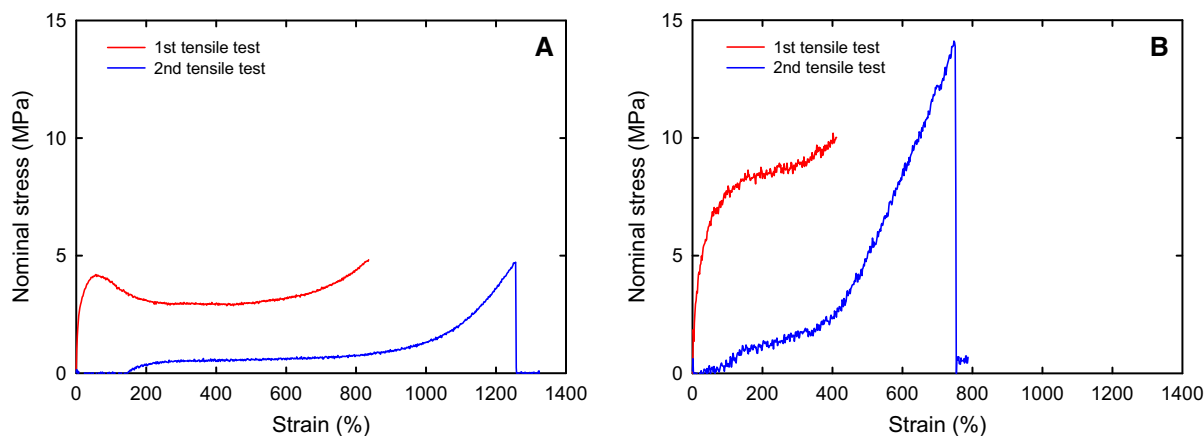
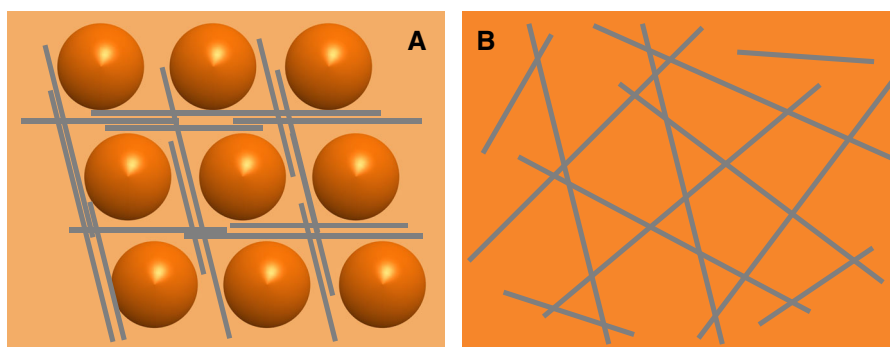


Fig. 9 Stress–strain curves for TOCN- $N(n\text{-Bu})_4$ /H-NBR (TOCN/H-NBR = 5/100, w/w) composite films prepared in heterogeneous system with water (a) and homogeneous system with DMF (b), obtained from first and second tensile tests

Fig. 10 Schematic structural models of TOCN- $N(n\text{-Bu})_4$ /H-NBR composite films prepared in heterogeneous system with water (a) (Fukui et al. 2018) and homogeneous system with DMF (b)



nanofiller effect on the composite materials. It is therefore necessary to establish suitable procedures for preparing TOCN/H-NBR composite films without using any organic solvent, to enable homogeneous distribution of TOCN elements in the homogeneous H-NBR polymer matrix, resulting in the TOCNs acting as efficient nanofillers in the composite films.

Conclusions

Composite films consisting of surface-hydrophobized TOCN- $N(n\text{-Bu})_4$ and H-NBR (TOCN/H-NBR = 0–5, w/w) were prepared in a heterogeneous system with water and a homogeneous system with DMF, by mixing, casting, and drying. The two composite films both had high Young's moduli of ~ 45 MPa and low CTEs of ~ 20 ppm/K at a weight ratio of TOCN/H-NBR = 5/100, irrespective of the system used to prepare the composite films. In contrast, the tensile

strengths and strain-to-failure values of composite films prepared using the two systems clearly differed. These common and different properties of the composite films prepared in the two systems are probably the results of different distributions/structures of the two components. The composite films prepared in the heterogeneous system with water partly retain the original latex particle structure and the TOCN elements are present in the films, surrounding the latex particles. In contrast, the composite films prepared in the homogeneous system with DMF have more homogeneous distributions of TOCN elements in the homogeneous H-NBR polymer matrix. Although the TOCN surfaces were hydrophobized with tetra-*n*-butylammonium groups, heterogeneous distribution of TOCN elements without penetration into the hydrophobic H-NBR molecules may be partly retained in the composite films.

Acknowledgments This research was supported by Core Research for Evolutional Science and Technology (CREST, Grant Number JPMJCR13B2) of the Japan Science and Technology Agency (JST). We thank Helen McPherson, Ph.D., from Edanz Group (www.edanzediting.com/ac) for editing a draft of this manuscript.

References

- Abraham E, Deepa B, Pothan LA, John M, Narine SS, Thomas S, Anandjiwala R (2013) Physicomechanical properties of nanocomposites based on cellulose nanofibre and natural rubber latex. *Cellulose* 20:417–427. <https://doi.org/10.1007/s10570-012-9830-1>
- Aimura Y (1997) Fundamental properties and applications of hydrogenated nitrile rubber. *Nippon Gomu Kyokaishi* 70:681–688. <https://doi.org/10.2324/gomu.70.681>
- Annamalai PK, Dagnon KL, Monemian S, Foster EJ, Rowan SJ, Weder C (2014) Water-responsive mechanically adaptive nanocomposites based on styrene-butadiene rubber and cellulose nanocrystals—processing matters. *ACS Appl Mater Interfaces* 6:967–976. <https://doi.org/10.1021/am404382x>
- Bendahou A, Kaddami H, Dufresne A (2010) Investigation on the effect of cellulosic nanoparticles' morphology on the properties of natural rubber based nanocomposites. *Eur Polym J* 46:609–620. <https://doi.org/10.1016/j.eurpolymj.2009.12.025>
- Bras J, Hassan ML, Bruzesse C, Hassan EA, El-Wakil NA, Dufresne A (2010) Mechanical, barrier, and biodegradability properties of bagasse cellulose whiskers reinforced natural rubber nanocomposites. *Ind Crops Prod* 32:627–633. <https://doi.org/10.1016/j.indcrop.2010.07.018>
- Brüning M (1998) Numerical analysis of modeling of large deformation and necking behavior of tensile specimens. *Finite Elem Anal Des* 28:303–319. [https://doi.org/10.1016/S0168-874X\(97\)00042-5](https://doi.org/10.1016/S0168-874X(97)00042-5)
- Bucknall CB, Smith RR (1965) Stress-whitening in high-impact polystyrenes. *Polymer* 6:437–446. [https://doi.org/10.1016/0032-3861\(65\)90028-5](https://doi.org/10.1016/0032-3861(65)90028-5)
- De SK, White JR (1996) Short fibre-polymer composites. Woodhead Publishing, Cambridge. ISBN 1-85573-220-3
- Deng F, Ito M, Noguchi T, Wang L, Ueki H, Niihara KI, Kim YA, Endo M, Zeng QS (2011) Elucidation of the reinforcing mechanism in carbon nanotube/rubber nanocomposites. *ACS Nano* 5:3858–3866. <https://doi.org/10.1021/nn200201u>
- Endo M, Noguchi T, Ito M, Takeuchi K, Hayashi T, Kim YA, Wanibuchi T, Jinnai H, Terrones M, Dresselhaus MS (2008) Extreme-performance rubber nanocomposites for probing and excavating deep oil resources using multi-walled carbon nanotubes. *Adv Funct Mater* 18:3403–3409. <https://doi.org/10.1002/adfm.200801136>
- Fujisawa S, Ikeuchi T, Takeuchi M, Saito T, Isogai A (2012a) Superior reinforcement effect of TEMPO-oxidized cellulose nanofibrils in polystyrene matrix: optical, thermal, and mechanical studies. *Biomacromolecules* 13:2188–2194. <https://doi.org/10.1021/bm300609c>
- Fujisawa S, Saito T, Kimura S, Iwata T, Isogai A (2012b) Surface engineering of ultrafine cellulose nanofibrils toward polymer nanocomposite materials. *Biomacromolecules* 14:1541–1546. <https://doi.org/10.1021/bm400178m>
- Fujisawa S, Saito T, Kimura S, Iwata T, Isogai A (2014) Comparison of mechanical reinforcement effects of surface-modified cellulose nanofibrils and carbon nanotubes in PLLA composites. *Compos Sci Technol* 90:96–101. <https://doi.org/10.1016/j.compscitech.2013.10.021>
- Fukui S, Ito T, Saito T, Noguchi T, Isogai A (2018) Counterion design of TEMPO-nanocellulose used as filler to improve properties of hydrogenated acrylonitrile-butadiene matrix. *Compos Sci Technol* 167:339–345. <https://doi.org/10.1016/j.compscitech.2018.08.023>
- Fukuzumi H, Saito T, Iwata T, Kumamoto Y, Isogai A (2009) Transparent and high gas barrier films of cellulose nanofibers prepared by TEMPO-mediated oxidation. *Biomacromolecules* 10:162–165. <https://doi.org/10.1021/bm801065u>
- Gatos KG, Százdí L, Pukánszky B, Karger-Kocsis J (2005) Controlling the deintercalation in hydrogenated nitrile rubber (HNBR)/organo-montmorillonite nanocomposite by curing with peroxide. *Macromol Rapid Commun* 26:915–919. <https://doi.org/10.1002/marc.200500084>
- Habibi Y, Lucian L, Rojas OJ (2010) Cellulose nanocrystals: chemistry, self-assembly, and applications. *Chem Rev* 110:3479–3500. <https://doi.org/10.1021/cr900339w>
- Haraguchi K, Ebato M, Takehisa T (2006) Polymer-clay nanocomposites exhibiting abnormal necking phenomena accompanied by extremely large reversible elongations and excellent transparency. *Adv Mater* 18:2250–2254. <https://doi.org/10.1002/adma.200600143>
- Hshim AS, Azahari B, Ikeda Y, Kohjiya S (1998) The effect of bis(3-triethoxysilylpropyl)tetrasulfide on silica reinforcement of styrene-butadiene rubber. *Rubber Chem Technol* 71:289–299. <https://doi.org/10.5254/1.3538485>
- Isogai A (2013) Wood nanocelluloses: fundamentals and applications as new bio-based nanomaterials. *J Wood Sci* 59:449–459. <https://doi.org/10.1007/s10086-013-1365-z>
- Isogai A, Saito T, Fukuzumi H (2011) TEMPO-oxidized cellulose nanofibers. *Nanoscale* 3:71–85. <https://doi.org/10.1039/c0nr00583e>
- Kader MA, Kim K, Lee YS, Nah C (2006) Preparation and properties of nitrile rubber/montmorillonite nanocomposites via latex blending. *J Mater Sci* 41:7341–7352. <https://doi.org/10.1007/s10853-006-0792-2>
- Karasek L, Sumita M (1996) Characterization of dispersion state of filler and polymer-filler interactions in rubber-carbon black composites. *J Mater Sci* 31:281–289. <https://doi.org/10.1007/BF01139141>
- Klemm D, Kramer F, Moritz S, Lindström T, Ankerfors M, Gray D, Dorris A (2011) Nanocelluloses: a new family of nature-based materials. *Angew Chem* 50:5438–5466. <https://doi.org/10.1002/anie.201001273>
- Moon RJ, Martini A, Nairn J, Simonsen J, Yungblood J (2011) Cellulose nanomaterials review: structure, properties and nanocomposites. *Chem Soc Rev* 40:3941–3994. <https://doi.org/10.1039/C0CS00108B>
- Nair KG, Dufresne A (2003) Crab shell chitin whisker reinforced natural rubber nanocomposites. 2. Mechanical

- behavior. *Biomacromolecules* 4:666–674. <https://doi.org/10.1021/bm0201284>
- Parambath Kanoth B, Claudino M, Johansson M, Berglund LA, Zhou Q (2015) Biocomposites from natural rubber: synergistic effects of functionalized cellulose nanocrystals as both reinforcing and cross-linking agents via free-radical thiol–ene chemistry. *ACS Appl Mater Interfaces* 7:16303–16310. <https://doi.org/10.1021/acsami.5b03115>
- Saito T, Nishiyama Y, Putaux JL, Vignon M, Isogai A (2006) Homogeneous suspensions of individualized microfibrils from TEMPO-catalyzed oxidation of native cellulose. *Biomacromolecules* 7:1687–1691. <https://doi.org/10.1021/bm060154s>
- Saito T, Kimura S, Nishiyama Y, Isogai A (2007) Cellulose nanofibers prepared by TEMPO-mediated oxidation of native cellulose. *Biomacromolecules* 8:2485–2491. <https://doi.org/10.1021/bm0703970>
- Shimizu M, Saito T, Isogai A (2014a) Bulky quaternary alkylammonium counterions enhance the nanodispersibility of 2,2,6,6-tetramethylpiperidine-1-oxyl-oxidized cellulose in diverse solvents. *Biomacromolecules* 15:1904–1909. <https://doi.org/10.1021/bm500384d>
- Shimizu M, Saito T, Fukuzumi H, Isogai A (2014b) Hydrophobic, ductile, and transparent nanocellulose films with quaternary alkylammonium carboxylates on nanofibril surfaces. *Biomacromolecules* 15:4320–4325. <https://doi.org/10.1021/bm501329v>
- Shimizu M, Saito T, Isogai A (2016) Water-resistant and high oxygen-barrier nanocellulose films with interfibrillar cross-linkages formed through multivalent metal ions. *J Membr Sci* 500:1–7. <https://doi.org/10.1021/bm2017542>
- Shinoda R, Saito T, Okita Y, Isogai A (2012) Relationship between length and degree of polymerization of TEMPO-oxidized cellulose nanofibrils. *Biomacromolecules* 13:842–849. <https://doi.org/10.1021/bm2017542>
- Soeta H, Fujisawa S, Saito T, Berglund L, Isogai A (2015) Low-birefringent and highly tough nanocellulose-reinforced cellulose triacetate. *ACS Appl Mater Interfaces* 7:11041–11046. <https://doi.org/10.1021/acsami.5b02863>
- Tervoort TA, Govaert LE (2000) Strain-hardening behavior of polycarbonate in the glassy state. *J Rheol* 44:1263–1277. <https://doi.org/10.1122/1.1319175>
- Varghese S, Karger-Kocsis J (2003) Natural rubber-based nanocomposites by latex compounding with layered silicates. *Polymer* 44:4921–4927. [https://doi.org/10.1016/S0032-3861\(03\)00480-4](https://doi.org/10.1016/S0032-3861(03)00480-4)
- Wang MJ (1998) Effect of polymer-filler and filler-filler interactions on dynamic properties of filled vulcanizates. *Rubber Chem Technol* 71:520–589. <https://doi.org/10.5254/1.3538492>
- Wu PD, van der Giessen E (1995) On neck propagation in amorphous glassy polymers under plane strain tension. *Int J Plast* 11:211–235. [https://doi.org/10.1016/0749-6419\(94\)00043-3](https://doi.org/10.1016/0749-6419(94)00043-3)